Scilight

Applied Mathematics and Statistics
https://www.sciltp.com/journals/ams

Article

Projective Synchronization of Quaternion-Valued Discontinuous Competitive Neural Networks with Multiple Time Scales

Yu Zheng, Ruoyu Wei * and Zixuan Chen

School of Mathematics and Statistics, Nanjing University of Information Science and Technology, Nanjing 210044, China
* Correspondence: ruoyuwei191@163.com

How To Cite: Zheng, Y.; Wei, R.; Chen, Z. Projective Synchronization of Quaternion-Valued Discontinuous Competitive Neural Networks with Multiple Time Scales. *Applied Mathematics and Statistics* **2025**, *2*(1), 2. https://doi.org/10.53941/ams.2025.100002.

Received: 28 March 2025
Revised: 18 April 2025
Accepted: 22 April 2025
Published: 24 April 2025

Abstract: In this study, we explore the projective synchronization of quaternion-valued competitive neural networks with multiple time scales (QVMTSCNNs), while analyzing the impacts of discontinuous activation functions and time delays. To achieve the control goal, two novel quaternion controllers are designed, which do not depend on the ratio of the fast and slow time scales. By applying the nonsmooth analysis and quaternion inequality techniques, two novel theorems for projective synchronization of QVMTSCNNs are derived by non-separating methods. The obtained results in this study are relatively simpler and straightforward, extending some previous findings. Lastly, numerical analyses are executed to substantiate the theoretical conclusions.

Keywords: projective synchronization; quaternion; competitive neural networks; multiple scales

1. Introduction

In recent decades, studies on real-valued neural networks (RVNNs) have made significant progress, while complex-valued neural networks (CVNNs) have also produced valuable results in many fields [1–4]. However, they have limitations in certain practical applications, especially in problems that involve handling high-dimensional data. To address these issues, quaternion-valued neural networks (QVNNs) were introduced as an important extension. QVNNs have shown great potential in areas such as wind speed forecasting, robot control, and aerospace engineering [5–7]. Due to the unique structure of quaternions, the dynamic behaviour of QVNNs is more complex than RVNNs and CVNNs. In the past, most studies on QVNNs have relied on decomposition methods [8–11], but these often lead to more complex derivations and may increase the conservatism of the results. Therefore, it is important to find a non-decomposition method with lower conservatism to study QVNNs.

Competitive Neural Networks (CNNs), an important category of neural networks, were first presented by Cohen and Grossberg in 1983 [12]. In the CNNs, there exist two different categories of change states. Short-term memory (STM) tracks rapid neural activity, while long-term memory (LTM) exhibits slow, unsupervised synaptic shifts. As research on competitive neural networks (CNNs) has progressed steadily, numerous important findings have emerged in the analysis of dynamic systems. Most researchers tend to focus on a single time scale when studying the dynamics of CNNs [13–15], while overlooking the fact that multiple time scales are more widespread during signal interactions among neural nodes. Therefore, the study of CNNs with multiple time scales can extend many previous works, making it a more meaningful area of research.

Although the dynamic characteristics of QVNNs and CNNs have been widely studied, there are still very few papers that combine the advantages of both. Existing research often focuses on their individual applications, such as the role of QVNNs in multi-dimensional signal processing [16], or the performance of CNNs in competitive dynamic models [17]. Few studies in the literature integrate both features, which limits the ability to deeply explore scenarios where high-dimensional data and competitive dynamics are present together. Therefore, this study introduces quaternion-valued competitive neural networks (QVCNNs), combining the strengths of both, and further expanding the potential of neural network models.

Synchronization, a vital dynamic property of neural networks, appears commonly in nature and remains a key

focus of research in recent years. In the 1990s, Pecora and Carroll were the first to investigate two chaotic systems with different initial conditions, proposing a synchronization method for drive-response systems [18]. This marked the beginning of a new era in the study of synchronization phenomena. Synchronization appears in diverse types, including complete synchronization [19], projective synchronization [20], and exponential synchronization [21], among others. Among them, projective synchronization is quite special because it can achieve various forms of synchronization by adjusting the proportional factor. It has shown better performance in fields like computer vision and medical imaging [22,23]. Furthermore, most previous studies treated the projective coefficient as real-valued. Compared to real-valued projective coefficients, quaternion-valued projective coefficients can enhance the diversity and complexity of synchronization, making the results more general.

When studying the synchronization of neural networks, we often encounter factors such as discontinuous activation functions and time delays. Discontinuous activation functions are common in complex systems. Unlike the smooth changes seen in traditional models, these functions can better reflect the dynamic behaviour of real networks [24]. Time delays refer to the lag in the feedback or input signals within the system, which can make the system's behaviour more complex, especially when multiple time scales are involved, potentially leading to phenomena like bifurcation and chaos [25]. Therefore, considering discontinuous activation functions and time delays plays a vital role in improving the robustness and real-world utility of neural networks.

Building on the preceding analysis, this study explores the projective synchronization of QVMTSCNNs. The primary contributions of this work are outlined below.

1. This research first incorporates multiple time scales into QVCNNs, which makes the dynamical behaviour more complex. The previous results in [13,26] can be seen as a particular circumstance of this paper.
2. We establish two innovative and succinct conditions to achieve projective synchronization of QVMTSCNNs using a non-separation approach. The results are represented by algebraic inequalities, which are easy to be verified.
3. Novel controllers for synchronization are formulated, independent of the time scale ratio, and designed to mitigate the ill-conditioned issue as the small parameter approaches zero.

Notations: $\widehat{\mathbb{R}}$, $\widehat{\mathbb{Q}}$, $\widehat{\mathbb{R}}^n$, and $\widehat{\mathbb{Q}}^n$ represent real numbers, quaternion numbers, n-dimensional real vector spaces, and n-dimensional quaternion vector spaces, respectively. Let $\widehat{I} = \{1, 2, \ldots, I\}$ and $\widehat{W} = \{1, 2, \ldots, W\}$. Consider $\Lambda = \Lambda^R + i\Lambda^I + j\Lambda^J + \hbar\Lambda^K \in \widehat{\mathbb{Q}}$, where $\Lambda^R, \Lambda^I, \Lambda^J, \Lambda^K \in \mathbb{R}$. Hamilton's rules state that $i^2 = j^2 = \hbar^2 = -1$ and $ij = \hbar$, $j\hbar = i$, $\hbar i = j$. $\overline{\Lambda}$, Λ^*, $||\Lambda||_1 = \sum_{\chi\in\{R,I,J,K\}} |\Lambda^\chi|$, $||\Lambda||_2 = \sqrt{\Lambda\overline{\Lambda}}$ denote the conjugate, the conjugate transpose, the 1-norm, and the 2-norm, respectively.

2. Preliminaries

Consider the QVCNNs model with multiple time scales as described below:

$$\begin{cases} STM: \epsilon\dot{x}_h(t) = -a_h x_h(t) + \sum_{s=1}^{I} b_{hs} f_s(x_s(t)) + E_h \sum_{j=1}^{W} \Upsilon_j z_{hj}(t) \\ \qquad\qquad + \sum_{s=1}^{I} c_{hs} f_s(x_s(t-\pi_s(t))), \\ LTM: \dot{z}_{hj}(t) = -d_h z_{hj}(t) + \Upsilon_j f_h(x_h(t)), \quad h, s \in \widehat{I}, j \in \widehat{W}. \end{cases} \tag{1}$$

where $x_h(t) \in \widehat{\mathbb{Q}}$ denotes the state variable of the hth neuron, $z_{hj}(t) \in \widehat{\mathbb{Q}}$ refers to the neuron's synaptic strength, $a_h > 0$ represents the self-regulation constant. The parameters $b_{hs}, c_{hs} \in \widehat{\mathbb{Q}}$ indicate the connection weights, $f_s(\cdot)$ is a discontinuous activation function. Υ_j is the external input, $d_h, E_h \in \widehat{\mathbb{R}}_+$ denote constants, ε indicates the time scale factor, the time delay $\pi_s(t)$ is such that $0 \le \pi_s(t) \le \widehat{\pi}$.

Define $P_h(t) = \sum_{j=1}^{W} \Upsilon_j z_{hj}(t)$ and $\Upsilon = (\Upsilon_1, \Upsilon_2, \ldots, \Upsilon_W)^T$, where Υ is normalized, i.e., $||\Upsilon||_2^2 = 1$. So, system (1) can be described by:

$$\begin{cases} STM: \epsilon\dot{x}_h(t) = -a_h x_h(t) + \sum_{s=1}^{I} b_{hs} f_s(x_s(t)) + E_h P_h(t) \\ \qquad\qquad + \sum_{s=1}^{I} c_{hs} f_s(x_s(t-\pi_s(t))), \\ LTM: \dot{P}_h(t) = -d_h P_h(t) + f_h(x_h(t)), \quad h \in \widehat{I}. \end{cases} \tag{2}$$

The initial conditions are listed below:

$$x_h(\tau) = A_h(\tau), \quad P_h(\tau) = B_h(\tau), \quad \tau \in [-\widehat{\pi}, 0], \quad h \in \widehat{I},$$

where $A_h(\tau), B_h(\tau)$ are continuous on $[-\widehat{\pi}, 0]$.

The slave system for Formula (2) is presented:

$$\begin{cases} STM: \epsilon \dot{y_h}(t) = -a_h y_h(t) + \sum_{s=1}^{I} b_{hs} f_s(y_s(t)) + E_h Q_h(t) \\ \qquad\qquad + \sum_{s=1}^{I} c_{hs} f_s(y_s(t-\pi_s(t))) + u_h(t), \\ LTM: \dot{Q}_h(t) = -d_h Q_h(t) + f_h(y_h(t)) + v_h(t), \quad h \in \widehat{I}. \end{cases} \tag{3}$$

In which $u_h(t), v_h(t)$ denote the controllers, $y_h(t), Q_h(t)$ are the response states of the hth neuron.

The initial conditions are stated as:

$$y_h(\tau) = \widetilde{A}_h(\tau), \quad Q_h(\tau) = \widetilde{B}_h(\tau), \quad \tau \in [-\widehat{\pi}, 0], \quad h \in \widehat{I},$$

where $\widetilde{A}_h(\tau), \widetilde{B}_h(\tau)$ are continuous on $[-\widehat{\pi}, 0]$.

The assumptions are as follows:

Assumption 1. *[15] For each $p \in \widehat{I}$, the function $f_p(x_p)$ can be expressed as:*

$$f_p(x_p) = f_p^R(x_p) + \imath f_p^I(x_p) + \jmath f_p^J(x_p) + \hbar f_p^K(x_p),$$

which is continuous except at a countable number of isolated points θ_p^l, where the limits $f_p^-(\theta_p^l)$ and $f_p^+(\theta_p^l)$ exist. Furthermore, the number of jump discontinuities of $f_p(x_p)$ within any bounded compact subset of $\widehat{\mathbb{Q}}$ is always finite.

Assumption 2. *For each $k \in \widehat{I}$, there are $L_k > 0$ and $H_k > 0$ such that:*

$$||Y_k - X_k||_l \leq L_k ||y_k - x_k||_l + H_k, \text{ and } ||f_k(x_k)||_l \leq M_k, \quad l = 1, 2,$$

holds for $x_k, y_k \in \widehat{\mathbb{Q}}$, $X_k \in \overline{co}[f_k(x_k)]$, $Y_k \in \overline{co}[f_k(y_k)]$. Here, $\overline{co}[f(\cdot)] = [\check{f}(\cdot), \hat{f}(\cdot)]$, where $\check{f}(\cdot)$ and $\hat{f}(\cdot)$ denote the minimum and maximum between $f^+(\cdot)$ and $f^-(\cdot)$, respectively.

For convenience, we provide the following definition:

Definition 1. *[4] A vector function $F(t)\colon [-\widehat{\pi}, T_0) \longrightarrow \widehat{\mathbb{Q}}^{2I}$, is defined as:*

$$F(t) = (x_1(t), x_2(t), \ldots, x_I(t), P_1(t), P_2(t), \ldots, P_I(t))^T,$$

$$\widetilde{F}(t) = (A_1(t), A_2(t), \ldots, A_I(t), B_1(t), B_2(t), \ldots, B_I(t))^T,$$

where $T_0 \in (0, +\infty)$, is defined as a Filippov solution to system (2) on the interval $[-\widehat{\pi}, T_0)$, if it meets these criteria:

(1) $F(t)$ exhibits absolute continuity in $[0, T_0)$;

(2) For the measurable function $X(t) = (X_1(t), X_2(t), \ldots, X_I(t))^T$ in $[0, T_0)$, satisfying $X_s \in \overline{co}[f_s(x_s(t))]$, then:

$$\begin{cases} STM: \epsilon \dot{x}_h(t) = -a_h x_h(t) + \sum_{s=1}^{I} b_{hs} X_s(t) + E_h P_h(t) \\ \qquad\qquad + \sum_{s=1}^{I} c_{hs} X_s(t-\pi_s(t)), \\ LTM: \dot{P}_h(t) = -d_h P_h(t) + X_h(t), \quad h \in \widehat{I}, \end{cases} \tag{4}$$

at almost every point t in $[0, T_0)$ (a.e.).

Comparable to system (2), there exists $Y_s(t) \in \overline{co}[f_s(y_s(t))]$, *we have:*

$$\begin{cases} STM: \epsilon \dot{y}_h(t) = -a_h y_h(t) + \sum_{s=1}^{I} b_{hs} Y_s(t) + E_h Q_h(t) \\ \qquad\qquad + \sum_{s=1}^{I} c_{hs} Y_s(t-\pi_s(t)) + u_h(t), \\ LTM: \dot{Q}_h(t) = -d_h Q_h(t) + Y_h(t) + v_h(t), \quad h \in \widehat{I}, \end{cases} \tag{5}$$

at almost every point t *in* $[0, T_0)$ *(a.e.).*

Let $e_h(t) = y_h(t) - \hat{\alpha}_h x_h(t), \sigma_h(t) = Q_h(t) - \hat{\alpha}_h P_h(t)$, *where* $\hat{\alpha}_h \in \widehat{\mathbb{Q}}$, $h \in \widehat{I}$, *denotes the projective synchronization error.*

Thus, the error system for Formulas (4) and (5) is:

$$\begin{cases} STM: \epsilon \dot{e}_h(t) = -a_h e_h(t) + \sum_{s=1}^{I} b_{hs}(Y_s(t) - \hat{\alpha}_h X_s(t)) \\ \qquad\qquad + \sum_{s=1}^{I} c_{hs}(Y_s(t-\pi_s(t)) - \hat{\alpha}_h X_s(t-\pi_s(t))) \\ \qquad\qquad + E_h \sigma_h(t) + u_h(t), \\ LTM: \dot{\sigma}_h(t) = -d_h \sigma_h(t) + Y_h(t) - \hat{\alpha}_h X_h(t) + v_h(t), \quad h \in \widehat{I}. \end{cases} \tag{6}$$

Definition 2. *Assume there are* $\hat{\alpha}_h \in \widehat{\mathbb{Q}}$ *that satisfies:*

$$\lim_{\tau \to +\infty} ||y_h(\tau) - \hat{\alpha}_h x_h(\tau)||_o = 0, \quad \lim_{\tau \to +\infty} ||Q_h(\tau) - \hat{\alpha}_h P_h(\tau)||_o = 0, \quad o = 1, 2,$$

the systems (4) and (5) achieve asymptotic projective synchronization with the coefficient $\hat{\alpha}_h$.

Remark 1. *When investigating projective synchronization, most studies have focused on projective coefficients within the real and complex domains [27–29]. In contrast, this paper considers projective coefficients in the quaternion domain, making the obtained results more general.*

Definition 3. *For any* $\theta = \theta^R + i\theta^I + j\theta^J + \hbar\theta^K \in \widehat{\mathbb{Q}}$, *the sign function of* θ *is given by:*

$$sgn(\theta) = sgn(\theta^R) + isgn(\theta^I) + jsgn(\theta^J) + \hbar sgn(\theta^K).$$

Lemma 1. [30] *For each* $h \in \widehat{I}$, *if* $x_h \geq 0$, *and* $0 \leq p \leq 1$, *then* $\sum_{h=1}^{I} x_h^p \geq (\sum_{h=1}^{I} x_h)^p$.

Lemma 2. [31] *Assume* $\mathcal{X} \in \widehat{\mathbb{Q}}^n$ *and* $\mathcal{Y} \in \widehat{\mathbb{Q}}^n$, *the following inequalities and identities hold:*

$$\begin{aligned} &(1)\mathcal{X}^* sgn(\mathcal{Y}) + sgn^*(\mathcal{Y})\mathcal{X} \\ &\quad \leq \mathcal{X}^* sgn(\mathcal{X}) + sgn^*(\mathcal{X})\mathcal{X} = 2||\mathcal{X}||_1, \\ &(2)D^+(\mathcal{X}^* sgn(\mathcal{X}) + sgn^*(\mathcal{X})\mathcal{X}) \\ &\quad = sgn^*(\mathcal{X})\dot{\mathcal{X}} + \mathcal{X}^* sgn(\dot{\mathcal{X}}), \quad ||\mathcal{X}||_1 \neq 0, \\ &(3)||\mathcal{X}\mathcal{Y}||_l \leq ||\mathcal{X}||_l ||\mathcal{Y}||_l, \quad l = 1, 2, \\ &(4)sgn^*(\mathcal{X})sgn(\mathcal{X}) = ||sgn(\mathcal{X})||_1, \\ &(5)\mathcal{X}^*\mathcal{Y} + \mathcal{Y}^*\mathcal{X} \leq \mathcal{X}^*\mathcal{X} + \mathcal{Y}^*\mathcal{Y}, \\ &(6)\mathcal{X}^*\mathcal{X} = ||\mathcal{X}||_2^2. \end{aligned}$$

Lemma 3. [32] *Consider* $V(\tau)$ *as a continuous positive-definite function that satisfies:*

$$\dot{V}(\tau) \leq -\zeta V(\tau)^\rho, \quad \forall \tau \geq 0, V(0) \geq 0,$$

where $\zeta > 0$, $0 < \rho < 1$. *Then,* $V(\tau)$ *approaches zero within a finite settling time* $T \leq \frac{V(0)^{1-\rho}}{\zeta(1-\rho)}$, *and* $V(\tau) \equiv 0$, $\forall \tau \geq T$.

3. Main Results

In this part, we develop two controllers and set rules to ensure that the systems (4) and (5) can achieve both asymptotic and finite-time projective synchronization.

3.1. Asymptotic Projective Synchronization of QVMTSCNNs

For the purpose of attaining asymptotic projective synchronization, the subsequent controllers are developed:

$$\begin{cases} u_h(t) = -\lambda_h e_h(t) - \mu_h \dfrac{e_h(t)}{||e_h(t)||_2} \\ v_h(t) = -\delta_h \sigma_h(t) - \beta_h \dfrac{\sigma_h(t)}{||\sigma_h(t)||_2}, \end{cases} \tag{7}$$

where $\lambda_h, \mu_h, \delta_h, \beta_h > 0$, and $h \in \widehat{I}$.

Theorem 1. *Based on Assumptions 1–2, the master-slave system* (4) *and* (5) *can achieve asymptotic projective synchronization with controller* (7)*, if there exist scalars A_h, B_h, C_h and D_h such that:*

$$A_h < 0, \quad B_h < 0, \quad C_h < 0, \quad D_h < 0, \tag{8}$$

where

$$\begin{aligned} A_h &= -2a_h + E_h + L_h - 2\lambda_h + \sum_{s=1}^{I} \left(L_s||b_{hs}||_2 + L_h||b_{hs}||_2\right), \\ B_h &= -2\mu_h + 2\sum_{s=1}^{I}(H_s + M_s(1 + ||\hat{\alpha}_h||_2)) \cdot ||b_{hs}||_2 \\ &\qquad + 2\sum_{s=1}^{I} M_s(1 + ||\hat{\alpha}_h||_2) \cdot ||c_{hs}||_2, \\ C_h &= -2d_h + L_h + E_h - 2\delta_h, \\ D_h &= 2H_h + M_h(1 + ||\hat{\alpha}_h||_2) - \beta_h, \quad h \in \widehat{I}. \end{aligned}$$

Proof. Select the Lyapunov functional:

$$V(t) = V_1(t) + V_2(t)$$

$$V_1(t) = \epsilon \sum_{h=1}^{I} e_h^*(t) e_h(t), \qquad V_2(t) = \sum_{h=1}^{I} \sigma_h^*(t)\sigma_h(t). \tag{9}$$

First, consider $V_1(t)$

$$\begin{aligned} D^+V_1(t) =& \sum_{h=1}^{I} \epsilon \dot{e}_h^*(t) e_h(t) + \epsilon e_h^*(t)\dot{e}_h(t) \\ =& \sum_{h=1}^{I} \Big[-a_h e_h(t) + \sum_{s=1}^{I} b_{hs}(Y_s(t) - \hat{\alpha}_h X_s(t)) + E_h \sigma_h(t) \\ &+ \sum_{s=1}^{I} c_{hs}(Y_s(t - \pi_s(t)) - \hat{\alpha}_h X_s(t - \pi_s(t))) + u_h(t)\Big]^* e_h(t) \\ &+ \sum_{h=1}^{I} e_h^*(t)\Big[-a_h e_h(t) + \sum_{s=1}^{I} b_{hs}(Y_s(t) - \hat{\alpha}_h X_s(t)) \\ &+ \sum_{s=1}^{I} c_{hs}(Y_s(t - \pi_s(t)) - \hat{\alpha}_h X_s(t - \pi_s(t))) + E_h \sigma_h(t) + u_h(t)\Big] \\ =& -2\sum_{h=1}^{I} a_h e_h^*(t) e_h(t) + \sum_{h=1}^{I} [u_h^*(t) e_h(t) + e_h^*(t) u_h(t)] \end{aligned}$$

$$
\begin{aligned}
&+\sum_{h=1}^{I}\sum_{s=1}^{I}(Y_s(t)-\hat{\alpha}_h X_s(t))^* b_{hs}^* e_h(t)+e_h^*(t)b_{hs}(Y_s(t)-\hat{\alpha}_h X_s(t))\\
&+\sum_{h=1}^{I}\sum_{s=1}^{I}(Y_s(t-\pi_s(t))-\hat{\alpha}_h X_s(t-\pi_s(t)))^* c_{hs}^* e_h(t)\\
&\qquad\qquad +e_h^*(t)c_{hs}(Y_s(t-\pi_s(t))-\hat{\alpha}_h X_s(t-\pi_s(t)))\\
&+\sum_{h=1}^{I}E_h\left[\sigma_h^*(t)e_h(t)+e_h^*(t)\sigma_h(t)\right].
\end{aligned}
$$

By Lemma 2, one gets

$$
-2\sum_{h=1}^{I}a_h e_h^*(t)e_h(t)=-2\sum_{h=1}^{I}a_h||e_h(t)||_2^2. \tag{10}
$$

With reference to Assumptions 1–2 and Lemma 2, we obtain

$$
\begin{aligned}
&\sum_{h=1}^{I}\sum_{s=1}^{I}(Y_s(t)-\hat{\alpha}_h X_s(t))^* b_{hs}^* e_h(t)+e_h^*(t)b_{hs}(Y_s(t)-\hat{\alpha}_h X_s(t))\\
=&\sum_{h=1}^{I}\sum_{s=1}^{I}\left[f_s(y_s(t)-f_s(\hat{\alpha}_h x_s(t))+f_s(\hat{\alpha}_h x_s(t))-\hat{\alpha}_h f_s(x_s(t))\right]^* b_{hs}^* e_h(t)\\
&\qquad +e_h^*(t)b_{hs}\left[f_s(y_s(t)-f_s(\hat{\alpha}_h x_s(t))+f_s(\hat{\alpha}_h x_s(t))-\hat{\alpha}_h(f_s(x_s(t))\right]\\
\le&2\sum_{h=1}^{I}\sum_{s=1}^{I}||[f_s(y_s(t))-f_s(\hat{\alpha}_h x_s(t))+f_s(\hat{\alpha}_h x_s(t))-\hat{\alpha}_h f_s(x_s(t))]b_{hs}||_2\cdot||e_h(t)||_2\\
\le&2\sum_{h=1}^{I}\sum_{s=1}^{I}||f_s(y_s(t))-f_s(\hat{\alpha}_h x_s(t))||_2\cdot||b_{hs}||_2\cdot||e_h(t)||_2\\
&\qquad +||f_s(\hat{\alpha}_h x_s(t))-\hat{\alpha}_h f_s(x_s(t))||_2\cdot||b_{hs}||_2\cdot||e_h(t)||_2\\
\le&2\sum_{h=1}^{I}\sum_{s=1}^{I}(L_s||e_s(t)||_2+H_s)\cdot||b_{hs}||_2\cdot||e_h(t)||_2\\
&\qquad +M_s(1+||\hat{\alpha}_h||_2)\cdot||b_{hs}||_2\cdot||e_h(t)||_2\\
\le&2\sum_{h=1}^{I}\sum_{s=1}^{I}\frac{1}{2}\cdot L_s\left(||e_s(t)||_2^2+||e_h(t)||_2^2\right)\cdot||b_{hs}||_2\\
&\qquad +(H_s+M_s(1+||\hat{\alpha}_h||_2))\cdot||b_{hs}||_2\cdot||e_h(t)||_2\\
=&\sum_{h=1}^{I}\sum_{s=1}^{I}L_h\cdot||b_{hs}||_2\cdot||e_h(t)||_2^2+\sum_{h=1}^{I}\sum_{s=1}^{I}L_s\cdot||b_{hs}||_2\cdot||e_h(t)||_2^2\\
&\qquad +2\sum_{h=1}^{I}\sum_{s=1}^{I}(H_s+M_s(1+||\hat{\alpha}_h||_2))\cdot||b_{hs}||_2\cdot||e_h(t)||_2,
\end{aligned}
\tag{11}
$$

similarly

$$
\begin{aligned}
&\sum_{h=1}^{I}\sum_{s=1}^{I}(Y_s(t-\pi_s(t))-\hat{\alpha}_h X_s(t-\pi_s(t)))^* c_{hs}^* e_h(t)\\
&\qquad +e_h^*(t)c_{hs}(Y_s(t-\pi_s(t))-\hat{\alpha}_h X_s(t-\pi_s(t)))\\
\le&2\sum_{h=1}^{I}\sum_{s=1}^{I}||f_s(y_s(t-\pi_s(t)))-\hat{\alpha}_h f_s(x_s(t-\pi_s(t)))||_2\cdot||c_{hs}||_2\cdot||e_h(t)||_2\\
\le&2\sum_{h=1}^{I}\sum_{s=1}^{I}M_s(1+||\hat{\alpha}_h||_2)\cdot||c_{hs}||_2\cdot||e_h(t)||_2,
\end{aligned}
\tag{12}
$$

and

$$\sum_{h=1}^{I} E_h[\sigma_h^*(t)e_h(t) + e_h^*(t)\sigma_h(t)] \leq \sum_{h=1}^{I} E_h\big(||e_h(t)||_2^2 + ||\sigma_h(t)||_2^2\big), \tag{13}$$

and

$$\begin{aligned}
&\sum_{h=1}^{I} u_h^*(t)e_h(t) + e_h^*(t)u_h(t) \\
=&\sum_{h=1}^{I} \big(- \lambda_h e_h(t) - \mu_h \frac{e_h(t)}{||e_h(t)||_2}\big)^* e_h(t) + e_h^*(t)\big(- \lambda_h e_h(t) - \mu_h \frac{e_h(t)}{||e_h(t)||_2}\big) \\
=&-2\sum_{h=1}^{I} \big(\lambda_h ||e_h(t)||_2^2 + \mu_h ||e_h(t)||_2\big) .
\end{aligned} \tag{14}$$

Moreover, for $V_2(t)$:

$$\begin{aligned}
D^+V_2(t) =& \sum_{h=1}^{I} \dot{\sigma}_h^*(t)\sigma_h(t) + \sigma_h^*(t)\dot{\sigma}_h(t) \\
=& \sum_{h=1}^{I} (-d_h\sigma_h(t) + Y_h(t) - \hat{\alpha}_h X_h(t) + v_h(t))^*\sigma_h(t) \\
&+ \sigma_h^*(t)(-d_h\sigma_h(t) + Y_h(t) - \hat{\alpha}_h X_h(t) + v_h(t)) \\
=& -2\sum_{h=1}^{I} d_h\sigma_h^*(t)\sigma_h(t) + \sum_{h=1}^{I} v_h^*(t)\sigma_h(t) + \sigma_h^*(t)v_h(t) \\
&+ \sum_{h=1}^{I} (Y_h(t) - \hat{\alpha}_h X_h(t))^*\sigma_h(t) + \sigma_h^*(t)(Y_h(t) - \hat{\alpha}_h X_h(t)),
\end{aligned}$$

similarly

$$-2\sum_{h=1}^{I} d_h\sigma_h^*(t)\sigma_h(t) = -2\sum_{h=1}^{I} d_h||\sigma_h(t)||_2^2, \tag{15}$$

and

$$\begin{aligned}
&\sum_{h=1}^{I} (Y_h(t) - \hat{\alpha}_h X_h(t))^*\sigma_h(t) + \sigma_h^*(t)(Y_h(t) - \hat{\alpha}_h X_h(t)) \\
\leq& 2\sum_{h=1}^{I} ||(Y_h(t) - \hat{\alpha}_h X_h(t))||_2 \cdot ||\sigma_h(t)||_2 \\
\leq& 2\sum_{h=1}^{I} (L_h \cdot ||e_h(t)||_2 + H_h + M_h(1 + ||\hat{\alpha}_h||_2)) \cdot ||\sigma_h(t)||_2 \\
=& 2\sum_{h=1}^{I} L_h \cdot ||e_h(t)||_2 \cdot ||\sigma_h(t)||_2 + (H_h + M_h(1 + ||\hat{\alpha}_h||_2)) \cdot ||\sigma_h(t)||_2 \\
\leq& \sum_{h=1}^{I} L_h(||e_h(t)||_2^2 + ||\sigma_h(t)||_2^2) + 2\sum_{h=1}^{I} (H_h + M_h(1 + ||\hat{\alpha}_h||_2)) \cdot ||\sigma_h(t)||_2,
\end{aligned} \tag{16}$$

and

$$\begin{aligned}
&\sum_{h=1}^{I} v_h^*(t)\sigma_h(t) + \sigma_h^*(t)v_h(t) \\
=& \sum_{h=1}^{I} \big(- \delta_h\sigma_h(t) - \beta_h \frac{\sigma_h(t)}{||\sigma_h(t)||_2}\big)^*\sigma_h(t) + \sigma_h^*(t)\big(- \delta_h\sigma_h(t) - \beta_h \frac{\sigma_h(t)}{||\sigma_h(t)||_2}\big)
\end{aligned}$$

$$= -2\sum_{h=1}^{I}(\delta_h||\sigma_h(t)||_2^2 + \beta_h||\sigma_h(t)||_2). \tag{17}$$

Combining the above Formulas (10)–(17), we obtain:

$$\begin{aligned}
D^+V(t) \leq & -2\sum_{h=1}^{I} a_h||e_h(t)||_2^2 - 2\sum_{h=1}^{I}(\delta_h||\sigma_h(t)||_2^2 + \beta_h||\sigma_h(t)||_2) \\
& + \sum_{h=1}^{I}\sum_{s=1}^{I} L_s \cdot ||b_{hs}||_2 \cdot ||e_h(t)||_2^2 + \sum_{h=1}^{I}\sum_{s=1}^{I} L_h \cdot ||b_{hs}||_2 \cdot ||e_h(t)||_2^2 \\
& + 2\sum_{h=1}^{I}\sum_{s=1}^{I}(H_s + M_s(1 + ||\hat{\alpha}_h||_2)) \cdot ||b_{hs}||_2 \cdot ||e_h(t)||_2 \\
& + 2\sum_{h=1}^{I}\sum_{s=1}^{I} M_s(1 + ||\hat{\alpha}_h||_2) \cdot ||c_{hs}||_2 \cdot ||e_h(t)||_2 - 2\sum_{h=1}^{I} d_h||\sigma_h(t)||_2^2 \\
& + \sum_{h=1}^{I} E_h(||e_h(t)||_2^2 + ||\sigma_h(t)||_2^2) - 2\sum_{h=1}^{I}(\lambda_h||e_h(t)||_2^2 + \mu_h||e_h(t)||_2) \\
& + \sum_{h=1}^{I} L_h(||e_h(t)||_2^2 + ||\sigma_h(t)||_2^2) \\
& + 2\sum_{h=1}^{I}(H_h + M_h(1 + ||\hat{\alpha}_h||_2)) \cdot ||\sigma_h(t)||_2 \\
= & \sum_{h=1}^{I} A_h||e_h(t)||_2^2 + \sum_{h=1}^{I} B_h||e_h(t)||_2 \\
& + \sum_{h=1}^{I} C_h||\sigma_h(t)||_2^2 + \sum_{h=1}^{I} D_h||\sigma_h(t)||_2.
\end{aligned}$$

Let $0 < G \leq \min\{-\frac{A_h}{\epsilon}, -C_h\}$, then, according to inequalities Formula (8). We have:

$$D^+V(t) \leq \sum_{h=1}^{I} A_h||e_h(t)||_2^2 + \sum_{h=1}^{I} C_h||\sigma_h(t)||_2^2 \leq -GV(t). \tag{18}$$

By integrating both sides of Equation (18) and considering the limit as $t \to +\infty$, we obtain the following result:

$$\lim_{t\to+\infty} V(t) \leq \lim_{t\to+\infty} C'e^{-Gt} = 0, \quad C' \in \widetilde{\mathbb{R}}. \tag{19}$$

Combining the aforementioned discussions, then:

$$\lim_{t\to+\infty} ||y_h(t) - \hat{\alpha}_h x_h(t)||_2 = 0, \lim_{t\to+\infty} ||S_h(t) - \hat{\alpha}_h R_h(t)||_2 = 0. \tag{20}$$

By Definition 2, the master-slave systems (4) and (5) achieve asymptotic projective synchronization. The proof is finished. □

Remark 2. *Notably, choosing different projective coefficients $\hat{\alpha}_h$ results in varying synchronization forms between Formulas (4) and (5). Specifically, when $\hat{\alpha}_h = 1$, projective synchronization becomes identical to complete synchronization. Conversely, when $\hat{\alpha}_h = -1$, it transforms into anti-synchronization.*

Remark 3. *When discussing the dynamical properties of QVNNs, many papers employ decomposition techniques [3,33,34], which generally involve more complex derivations. However, in this paper, we fully utilize the properties of quaternions and use a non-decomposition approach, thereby reducing conservatism.*

Remark 4. *Unlike the Lyapunov function constructed in [13], we construct an ϵ-dependent composite Lyapunov function based on time scales, which significantly reduces the computational load associated with differentiation.*

3.2. Finite-Time Projective Synchronization of QVMTSCNNs

To realize finite-time projective synchronization, the following controllers are developed:

$$\begin{cases} u_h(t) = -\eta_h e_h(t) - \Theta_h sgn(e_h(t)) - \gamma_h sgn(e_h(t))||e_h(t)||_1^\rho \\ v_h(t) = -\kappa_h \sigma_h(t) - \Omega_h sgn(\sigma_h(t)) - \iota_h sgn(\sigma_h(t))||\sigma_h(t)||_1^\rho, \end{cases} \tag{21}$$

where $\eta_h, \gamma_h, \kappa_h, \iota_h, \Theta_h, \Omega_h > 0, 0 < \rho < 1$, and $h \in \widehat{I}$.

Theorem 2. *Given Assumptions 1–2, the system described by systems* (4) *and* (5) *can attain finite-time projective synchronization using the controller* (21)*, provided the following inequalities hold:*

$$\begin{aligned} \sum_{h=1}^{I}\sum_{s=1}^{I}[(H_s + M_s(1+||\hat{\alpha}_h||_1)) \cdot ||b_{hs}||_1 + M_s(1+||\hat{\alpha}_h||_1) \cdot ||c_{hs}||_1] \\ + \sum_{h=1}^{I}[H_h + M_h(1+||\hat{\alpha}_h||_1)] \leq \sum_{h=1}^{I}(\Theta_h + \Omega_h), \\ -a_h + \sum_{s=1}^{I} L_h \cdot ||b_{hs}||_1 + L_h \leq \eta_h, \quad E_h - d_h \leq \kappa_h, \quad h \in \widehat{I}. \end{aligned} \tag{22}$$

One can estimate the setting time by :

$$T_1 \leq \frac{\left(\sum_{h=1}^{I} \epsilon||e_h(0)||_1 + \sum_{h=1}^{I} ||\sigma_h(0)||_1\right)^{1-\rho}}{F(1-\rho)},$$

where $0 < F \leq \min\{\frac{\gamma_i}{\epsilon}, \iota_i\}$.

Proof. Consider the following Lyapunov functional:

$$V(t) = V_1(t) + V_2(t)$$

$$\begin{cases} V_1(t) = \frac{\epsilon}{2}\sum_{h=1}^{I}(sgn^*(e_h(t))e_h(t) + e_h^*(t)sgn(e_h(t))) \\ V_2(t) = \frac{1}{2}\sum_{h=1}^{I}(sgn^*(\sigma_h(t))\sigma_h(t) + \sigma_h^*(t)sgn(\sigma_h(t))) \end{cases} \tag{23}$$

First, consider $V_1(t)$:

$$\begin{aligned} D^+V_1(t) =& \frac{\epsilon}{2}\sum_{h=1}^{I}(sgn^*(e_h(t))\dot{e}_h(t) + \dot{e}_h^*(t)sgn(e_h(t))) \\ =& \frac{1}{2}\sum_{h=1}^{I} sgn^*(e_h(t))\big[-a_h e_h(t) + \sum_{s=1}^{I} b_{hs}(Y_s(t) - \hat{\alpha}_h X_s(t)) \\ &+ \sum_{s=1}^{I} c_{hs}(Y_s(t-\pi_s(t)) - \hat{\alpha}_h X_s(t-\pi_s(t))) + E_h\sigma_h(t) + u_h(t)\big] \\ &+ \frac{1}{2}\sum_{h=1}^{I}\big[-a_h e_h(t) + \sum_{s=1}^{I} c_{hs}(Y_s(t-\pi_s(t)) - \hat{\alpha}_h X_s(t-\pi_s(t))) \\ &+ \sum_{s=1}^{I} b_{hs}(Y_s(t) - \hat{\alpha}_h X_s(t)) + E_h\sigma_h(t) + u_h(t)\big]^* sgn(e_h(t)) \\ =& \sum_{h=1}^{I} -\frac{a_h}{2}[sgn^*(e_h(t))e_h(t) + e_h^*(t)sgn(e_h(t))] \end{aligned}$$

$$
\begin{aligned}
&+\frac{1}{2}\sum_{h=1}^{I}\sum_{s=1}^{I}[sgn^*(e_h(t))b_{hs}(Y_s(t)-\hat{\alpha}_h X_s(t))\\
&\qquad+(Y_s(t)-\hat{\alpha}_h X_s(t))^* b_{hs}^* sgn(e_h(t))]\\
&+\frac{1}{2}\sum_{h=1}^{I}\sum_{s=1}^{I}[sgn^*(e_h(t))c_{hs}(Y_s(t-\pi_s(t))-\hat{\alpha}_h X_s(t-\pi_s(t)))\\
&\qquad+(Y_s(t-\pi_s(t))-\hat{\alpha}_h X_s(t-\pi_s(t)))^* c_{hs}^* sgn(e_h(t))]\\
&+\frac{1}{2}\sum_{h=1}^{I}E_h\big[sgn^*(e_h(t))\sigma_h(t)+\sigma_h^*(t)sgn(e_h(t)))\big]\\
&+\frac{1}{2}\sum_{h=1}^{I}sgn^*(e_h(t))u_h(t)+u_h^*(t)sgn(e_h(t)).
\end{aligned}
$$

By Lemma 2, one has

$$
\sum_{h=1}^{I}-\frac{a_h}{2}[sgn^*(e_h(t))e_h(t)+e_h^*(t)sgn(e_h(t))]=-\sum_{h=1}^{I}a_h||e_h(t)||_1. \tag{24}
$$

The subsequent proof follows the same method as Theorem 1, and thus the calculation process is simplified

$$
\begin{aligned}
&\frac{1}{2}\sum_{h=1}^{I}\sum_{s=1}^{I}\big[sgn^*(e_h(t))b_{hs}(Y_s(t)-\hat{\alpha}_h X_s(t))+(Y_s(t)-\hat{\alpha}_h X_s(t))^* b_{hs}^* sgn(e_h(t)\big]\\
\le&\sum_{h=1}^{I}\sum_{s=1}^{I}\big[||f_s(y_s(t)-f_s(\hat{\alpha}_h x_s(t))||_1+||f_s(\hat{\alpha}x_s(t))-\hat{\alpha}_h f_s(x_s(t))||_1\big]\cdot||b_{hs}||_1\\
\le&\sum_{h=1}^{I}\sum_{s=1}^{I}\big[(L_s||e_s(t)||_1+H_s)+M_s(1+||\hat{\alpha}_h||_1)\big]\cdot||b_{hs}||_1\\
=&\sum_{h=1}^{I}\sum_{s=1}^{I}L_h\cdot||b_{hs}||_1\cdot||e_h(t)||_1+\sum_{h=1}^{I}\sum_{s=1}^{I}(H_s+M_s(1+||\hat{\alpha}_h||_1))\cdot||b_{hs}||_1,
\end{aligned} \tag{25}
$$

similarly

$$
\begin{aligned}
&\frac{1}{2}\sum_{h=1}^{I}\sum_{s=1}^{I}[sgn^*(e_h(t))c_{hs}(Y_s(t-\pi_s(t))-\hat{\alpha}_h X_s(t-\pi_s(t)))\\
&\qquad+(Y_s(t-\pi_s(t))-\hat{\alpha}_h X_s(t-\pi_s(t)))^* c_{hs}^* sgn(e_h(t))]\\
\le&\sum_{h=1}^{I}\sum_{s=1}^{I}||c_{hs}(Y_s(t-\pi_s(t))-\hat{\alpha}_h X_s(t-\pi_s(t)))||_1\\
\le&\sum_{h=1}^{I}\sum_{s=1}^{I}M_s(1+||\hat{\alpha}_h||_1)\cdot||c_{hs}||_1,
\end{aligned} \tag{26}
$$

and

$$
\frac{1}{2}\sum_{h=1}^{I}E_h[sgn^*(e_h(t))\sigma_h(t)+\sigma_h^*(t)sgn(e_h(t)))]\le\sum_{h=1}^{I}E_h||\sigma_h(t)||_1, \tag{27}
$$

and

$$
\begin{aligned}
&\frac{1}{2}\sum_{h=1}^{I}sgn^*(e_h(t))u_h(t)+u_h^*(t)sgn(e_h(t))\\
=&\frac{1}{2}\sum_{h=1}^{I}sgn^*(e_h(t))(-\eta_h e_h(t)-\Theta_h sgn(e_h(t))-\gamma_h sgn(e_h(t))||e_h(t)||_1^{\rho})
\end{aligned}
$$

$$
\begin{aligned}
&+(-\eta_h e_h(t)-\Theta_h sgn(e_h(t))-\gamma_h sgn(e_h(t))||e_h(t)||_1^{\rho})^* sgn(e_h(t))\\
\leq&\sum_{h=1}^{I}[-\eta_h||e_h(t)||_1-\gamma_h||sgn(e_h(t))||_1||e_h(t)||_1^{\rho}]-\sum_{h=1}^{I}\Theta_h. \qquad (28)
\end{aligned}
$$

Moreover, for $V_2(t)$:

$$
\begin{aligned}
D^+V_2(t)=&\frac{1}{2}\sum_{h=1}^{I}[sgn^*(\sigma_h(t))\dot{\sigma}_h(t)+\dot{\sigma}_h^*(t)sgn(\sigma_h(t))]\\
=&\frac{1}{2}\sum_{h=1}^{I}sgn^*(\sigma_h(t))(-d_h\sigma_h(t)+Y_h(t)-\hat{\alpha}_h X_h(t)+v_h(t))\\
&+(-d_h\sigma_h(t)+Y_h(t)-\hat{\alpha}_h X_h(t)+v_h(t))^* sgn(\sigma_h(t))\\
=&-\frac{1}{2}\sum_{h=1}^{I}d_h\left[sgn^*(\sigma_h(t))\sigma_h(t)+\sigma_h^*(t)sgn(\sigma_h(t))\right]\\
&+\frac{1}{2}\sum_{h=1}^{I}[sgn^*(\sigma_h(t))(Y_h(t)-\hat{\alpha}_h X_h(t))\\
&\qquad+(Y_h(t)-\hat{\alpha}_h X_h(t))^* sgn(\sigma_h(t))]\\
&+\frac{1}{2}\sum_{h=1}^{I}sgn^*(\sigma_h(t))v_h(t)+v_h^*(t)sgn(\sigma_h(t)),
\end{aligned}
$$

similarly

$$
-\frac{1}{2}\sum_{h=1}^{I}d_h[sgn^*(\sigma_h(t))\sigma_h(t)+\sigma_h^*(t)sgn(\sigma_h(t))]=-\sum_{h=1}^{I}d_h||\sigma_h(t)||_1, \qquad (29)
$$

and

$$
\begin{aligned}
&\sum_{h=1}^{I}\frac{1}{2}[sgn^*(\sigma_h(t))(Y_h(t)-\hat{\alpha}_h X_h(t))+(Y_h(t)-\hat{\alpha}_h X_h(t))^* sgn(\sigma_h(t))]\\
\leq&\sum_{h=1}^{I}||Y_h(t)-\hat{\alpha}_h X_h(t)||_1\leq\sum_{h=1}^{I}[(L_h||e_h(t)||_1+H_h)+M_h(1+||\hat{\alpha}_h||_1)], \qquad (30)
\end{aligned}
$$

and

$$
\begin{aligned}
&\frac{1}{2}\sum_{h=1}^{I}sgn^*(\sigma_h(t))v_h(t)+v_h^*(t)sgn(\sigma_h(t))\\
=&\frac{1}{2}\sum_{h=1}^{I}sgn^*(\sigma_h(t))(-\kappa_h\sigma_h(t)-\Omega_h sgn(\sigma_h(t))-\iota_h sgn(\sigma_h(t))||\sigma_h(t)||_1^{\rho})\\
&+(-\kappa_h\sigma_h(t)-\Omega_h sgn(\sigma_h(t))-\iota_h sgn(\sigma_h(t))||\sigma_h(t)||_1^{\rho})^* sgn(\sigma_h(t))\\
\leq&\sum_{h=1}^{I}[-\kappa_h||\sigma_h(t)||_1-\iota_h||sgn(\sigma_h(t))||_1||\sigma_h(t)||_1^{\rho}]-\sum_{h=1}^{I}\Omega_h. \qquad (31)
\end{aligned}
$$

By organizing the above Formulas (24)–(31) and inequalities (22), then:

$$
\begin{aligned}
D^+V(t)\leq&-\sum_{h=1}^{I}a_h||e_h(t)||_1+\sum_{h=1}^{I}\sum_{s=1}^{I}L_h\cdot||b_{hs}||_1\cdot||e_h(t)||_1-\sum_{h=1}^{I}\eta_h||e_h(t)||_1\\
&+\sum_{h=1}^{I}\sum_{s=1}^{I}(H_s+M_s(1+||\hat{\alpha}_h||_1))\cdot||b_{hs}||_1-\sum_{h=1}^{I}\kappa_h||\sigma_h(t)||_1\\
&+\sum_{h=1}^{I}\sum_{s=1}^{I}M_s(1+||\hat{\alpha}_h||_1)\cdot||c_{hs}||_1-\sum_{h=1}^{I}\iota_h||sgn(\sigma_h(t))||_1||\sigma_h(t)||_1^{\rho}
\end{aligned}
$$

$$
\begin{aligned}
&-\sum_{h=1}^{I}\gamma_h||sgn(e_h(t))||_1||e_h(t)||_1^{\rho}-\sum_{h=1}^{I}d_h||\sigma_h(t)||_1+\sum_{h=1}^{I}E_h||\sigma_h(t)||_1\\
&+\sum_{h=1}^{I}[(L_h||e_h(t)||_1+H_h)+M_h(1+||\hat{\alpha}_h||_1)]-\sum_{h=1}^{I}\Theta_h-\sum_{h=1}^{I}\Omega_h\\
\leq&-\gamma_h\sum_{h=1}^{I}||sgn(e_h(t))||_1||e_h(t)||_1^{\rho}-\iota_h\sum_{h=1}^{I}||sgn(\sigma_h(t))||_1||\sigma_h(t)||_1^{\rho}.
\end{aligned}
$$

According to lemma 1, and $||sgn(e_h(t))||_1$=0 or 1, $||sgn(\sigma_h(t))||_1$=0 or 1. let $0<F\leq\min\{\frac{\gamma_h}{\epsilon},\iota_h\}$, then:

$$
\begin{aligned}
D^+V(t)\leq&-F(\sum_{h=1}^{I}\epsilon||e_h(t)||_1^{\rho}+\sum_{h=1}^{I}||\sigma_h(t)||_1^{\rho})\\
\leq&-F(\sum_{h=1}^{I}\epsilon||e_h(t)||_1+\sum_{h=1}^{I}||\sigma_h(t)||_1)^{\rho}=-FV(t)^{\rho}.
\end{aligned}
$$

Using Lemma 3, the master-slave systems (4) and (5) can achieve finite-time projective synchronization, with the settling time estimated by:

$$
T_1\leq\frac{V(0)^{1-\rho}}{F(1-\rho)}=\frac{\left(\sum_{h=1}^{I}\epsilon||e_h(0)||_1+\sum_{h=1}^{I}||\sigma_h(0)||_1\right)^{1-\rho}}{F(1-\rho)}.
$$

We have completed the proof. □

Remark 5. *The synchronization of CNNs has been explored in* [14,35]*, yet these studies overlooked the impact of time delay. Since time delay is an inherent characteristic of neural networks, affecting their oscillatory behaviour, its consideration is essential.*

4. Numerical Simulation

This section demonstrates the validity of Theorems 1–2 through two examples.

Consider the QVMTSCNNs model:

$$
\begin{cases}
STM:\epsilon\dot{x}_h(t)=-a_hx_h(t)+\sum_{s=1}^{2}b_{hs}f_s(x_s(t))+E_hP_h(t)\\
\qquad\qquad+\sum_{s=1}^{2}c_{hs}f_s(x_s(t-\pi_s(t))),\\
LTM:\dot{P}_h(t)=-d_hP_h(t)+f_h(x_h(t)),\quad h=1,2.
\end{cases}
\tag{32}
$$

where $\epsilon=0.2, a_1=a_2=3, d_1=d_2=2.8, E_1=1.2, E_2=1$, and $\pi_s(t)=0.8\sin(t)+1.0$, $f_s(\theta)=0.1[(\sin(\theta^R)+0.01\text{sign}(\theta^R))+i(\sin(\theta^I)+0.01\text{sign}(\theta^I))+j(\sin(\theta^J)+0.01\text{sign}(\theta^J))+k(\sin(\theta^K)+0.01\text{sign}(\theta^K))]$.

$$
(b_{ij})_{2\times2}=\begin{pmatrix}0.61+1.02i-0.53j+0.32k & 0.94-0.71i+0.25j-0.63k\\ 0.10+0.75i-1.02j-0.88k & 1.43-0.22i-0.51j+0.39k\end{pmatrix},
$$

and

$$
(c_{ij})_{2\times2}=\begin{pmatrix}0.22+0.21i-0.14j-1.09k & 0.74-1.25i+0.75j-0.20k\\ 1.15-1.28i-0.26j+0.60k & 1.92+0.41i-1.83j+0.79k\end{pmatrix}.
$$

The slave system is defined as:

$$
\begin{cases}
STM:\epsilon\dot{y}_h(t)=-a_hy_h(t)+\sum_{s=1}^{2}b_{hs}f_s(y_s(t))+E_hQ_h(t)\\
\qquad\qquad+\sum_{s=1}^{2}c_{hs}f_s(y_s(t-\pi_s(t)))+u_h(t),\\
LTM:\dot{Q}_h(t)=-d_hQ_h(t)+f_h(y_h(t))+v_h(t),\quad h=1,2,
\end{cases}
\tag{33}
$$

the variables of system (33) are the same as those of system (32).

First, we show the asymptotic projective synchronization of the master-slave systems (32) and (33) using the controllers given below:

$$\begin{cases} u_h(t) = -\lambda_h e_h(t) - \mu_h \dfrac{e_h(t)}{||e_h(t)||_2} \\ v_h(t) = -\delta_h \sigma_h(t) - \beta_h \dfrac{\sigma_h(t)}{||\sigma_h(t)||_2}, \qquad h = 1, 2. \end{cases} \tag{34}$$

It is easy to compute that $L_1 = L_2 = 0.1, H_1 = H_2 = 0.02$, and $M_1 = M_2 = 0.404$. The projective coefficients are chosen $\hat{\alpha}_1 = 0.5 - 1.1i + 0.1j - 1.0k, \hat{\alpha}_2 = 1.4 + 0.3i + 0.7j - 0.3k$.

Taking the control parameters $\lambda_1 = \lambda_2 = 0.6, \mu_1 = \mu_2 = 7, \delta_1 = \delta_2 = 1.4, \beta_1 = \beta_2 = 1.2$. Then, all the requirements of Theorem 1 are met. Randomly select 6 sets of initial values. The systems (32) and (33) can achieve asymptotic projective synchronization with controller (34), which is shown in Figures 1 and 2.

Secondly, we show the finite-time projective synchronization of the master-slave systems (32) and (33) using the following controllers:

$$\begin{cases} u_h(t) = -\eta_h e_h(t) - \Theta_h sgn(e_h(t)) - \gamma_h sgn(e_h(t))||e_h(t)||_1^{\rho} \\ v_h(t) = -\kappa_h \sigma_h(t) - \Omega_h sgn(\sigma_h(t)) - \iota_h sgn(\sigma_h(t))||\sigma_h(t)||_1^{\rho}, \quad h = 1, 2. \end{cases} \tag{35}$$

Select $F = 0.5, \eta_1 = \eta_2 = 5, \kappa_1 = \kappa_2 = 2.5, \gamma_1 = \gamma_2 = 0.4, \iota_1 = \iota_2 = 0.6, \Theta_1 = \Theta_2 = 8, \Omega_1 = \Omega_2 = 4, \rho = 0.7$. Then, all criteria in Theorem 2 are satisfied. Randomly select 6 sets of initial values. Therefore, the systems (32) and (33) achieve finite-time projective synchronization with controller (35), as illustrated in Figures 3 and 4. The settling time is calculated as $T_1 = 7.6s$.

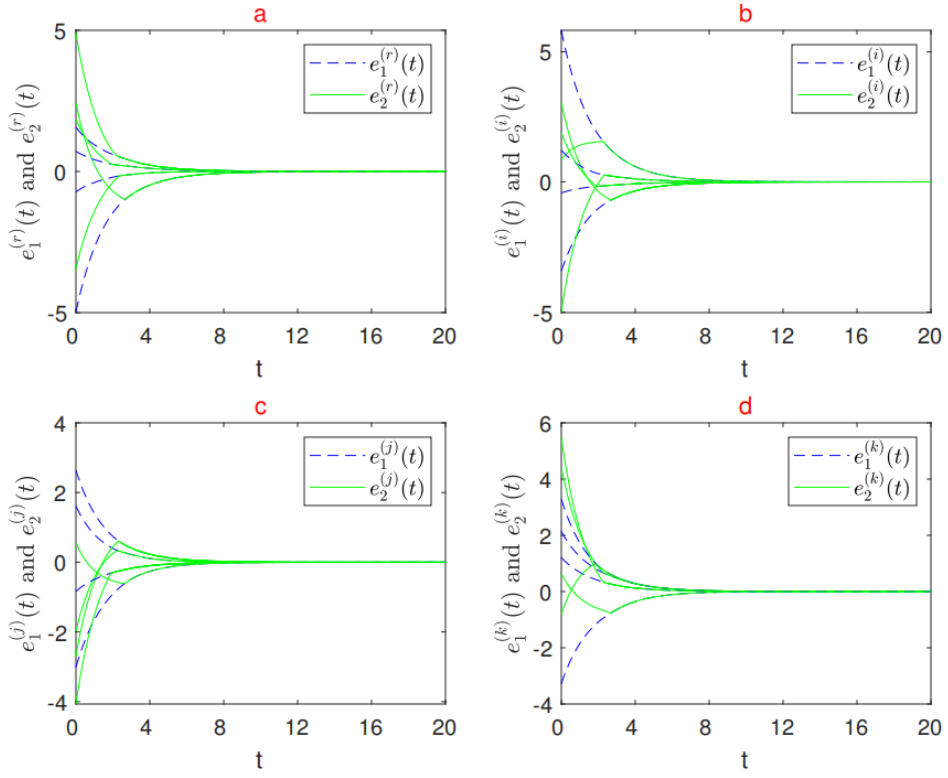

Figure 1. States of $e^r(t), e^i(t), e^j(t)$, and $e^k(t)$ of Systems (32) and (33) with controller (34).

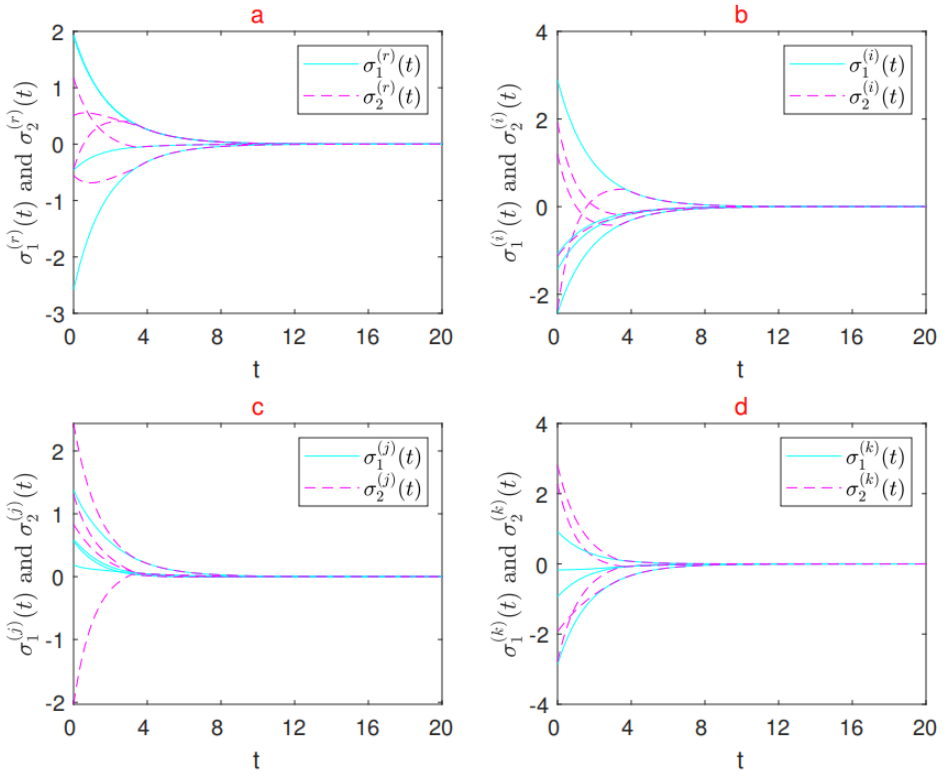

Figure 2. States of $\sigma^r(t), \sigma^i(t), \sigma^j(t)$, and $\sigma^k(t)$ of Systems (32) and (33) with controller (34).

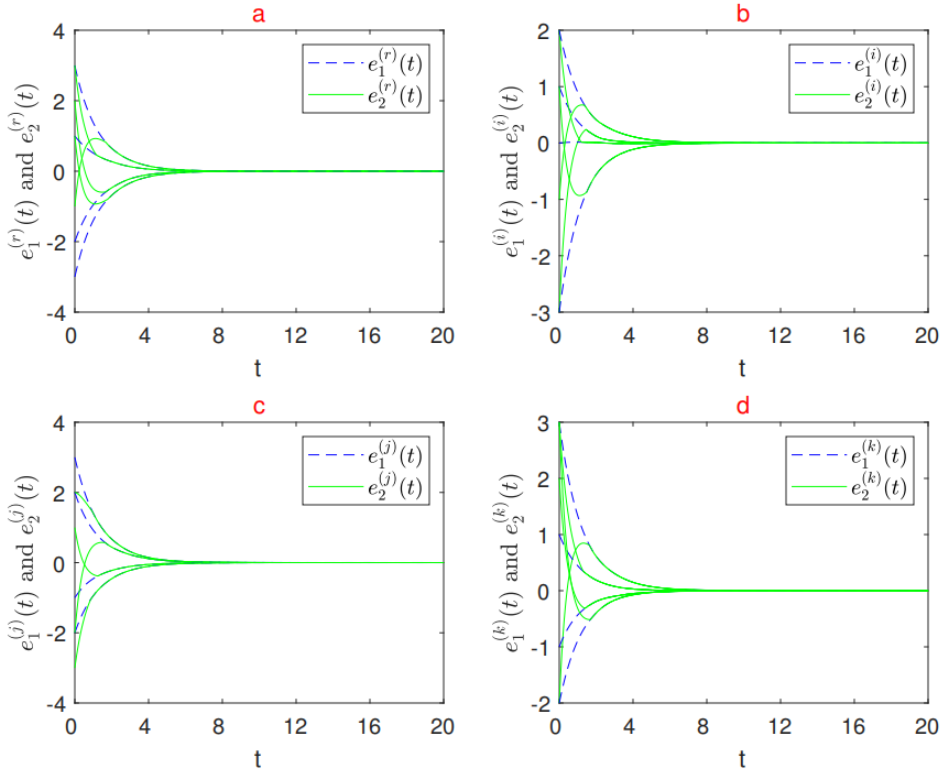

Figure 3. States of $e^r(t), e^i(t), e^j(t)$, and $e^k(t)$ of Systems (32) and (33) with controller (35).

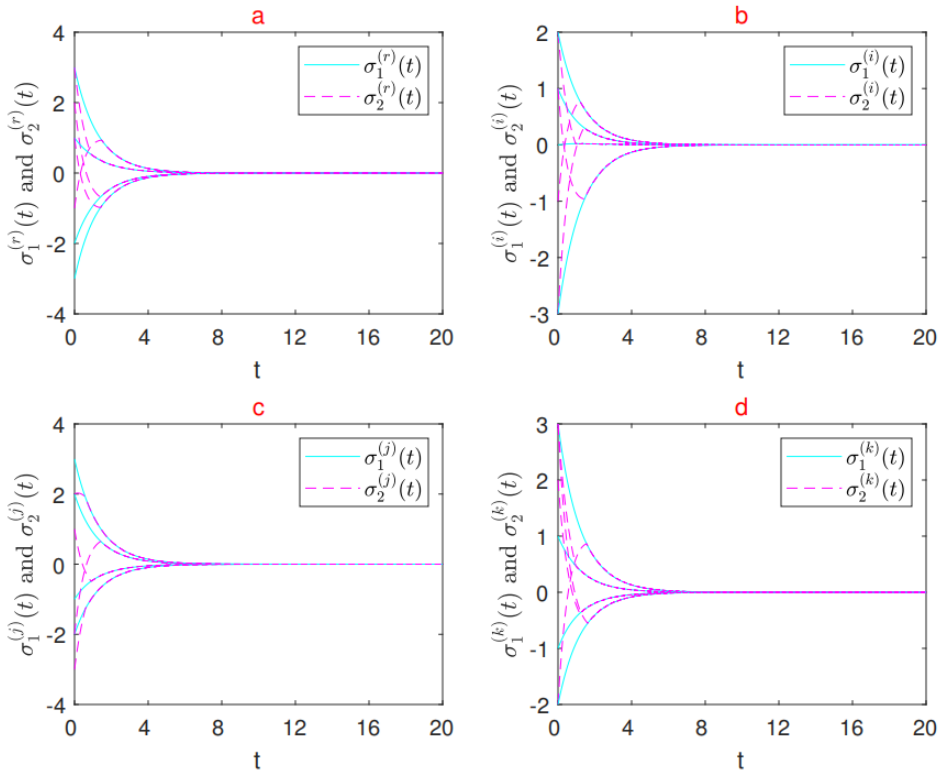

Figure 4. States of $\sigma^r(t), \sigma^i(t), \sigma^j(t)$, and $\sigma^k(t)$ of Systems (32) and (33) with controller (35).

5. Conclusions

This paper establishes a quaternion-valued competitive neural network model under multiple time scales (QVMTSCNNs) and investigates its asymptotic and finite-time projective synchronization problems. The results are validated through two numerical simulations. Future research will focus on exploring additional types of synchronization in QVMTSCNNs.

Author Contributions

Y.Z.: data curation, writing—original draft preparation; R.W.: conceptualization, methodology, supervision; Z.C.: visualization, writing—reviewing and editing. All authors have read and agreed to the published version of the manuscript.

Funding

This work is sponsored by National Natural Science Foundation of China (No. 12301625).

Data Availability Statement

Not applicable.

Conflicts of Interest

The authors declare no conflict of interest.

References

1. Guo, R.; Lu, J.; Li, Y.; et al. Fixed-time synchronization of inertial complex-valued neural networks with time delays. *Nonlinear Dyn.* **2021**, *105*, 1643–1656.
2. Chen, J.; Chen, B.; Zeng, Z. Global asymptotic stability and adaptive ultimate mittag–leffler synchronization for a fractional-order complex-valued memristive neural networks with delays. *IEEE Trans. Syst. Man Cybern. Syst.* **2018**, *49*, 2519–2535.
3. Chen, D.; Zhang, W.; Cao, J.; et al. Fixed time synchronization of delayed quaternion-valued memristor-based neural networks. *Adv. Differ. Equ.* **2020**, *2020*, 1–16.

4. Feng, L.; Hu, C.; Yu, J.; et al. Fixed-time synchronization of coupled memristive complex-valued neural networks. *Chaos Solitons Fractals* **2021**, *148*, 110993.
5. El Alami, A.; Berrahou, N.; Lakhili, Z.; et al. Efficient color face recognition based on quaternion discrete orthogonal moments neural networks. *Multimed. Tools Appl.* **2022**, *81*, 7685–7710.
6. Cui, Y.; Takahashi, K.; Hashimoto, M. Design of control systems using quaternion neural network and its application to inverse kinematics of robot manipulator. In Proceedings of the 2013 IEEE/SICE International Symposium on System Integration, Kobe, Japan, 15–17 December 2013; pp. 527–532.
7. Serrano, F.; Castillo, O.; Alassafi, M.; et al. Terminal sliding mode attitude-position quaternion based control of quadrotor unmanned aerial vehicle. *Adv. Space Res.* **2023**, *71*, 3855–3867.
8. Wei, W.; Yu, J.; Wang, L.; et al. Fixed/preassigned-time synchronization of quaternion-valued neural networks via pure power-law control. *Neural Netw.* **2022**, *146*, 341–349.
9. Zhang, J.; Ma, X.; Li, Y.; et al. Synchronization in fixed/preassigned-time of delayed fully quaternion-valued memristive neural networks via non-separation method. *Commun. Nonlinear Sci. Numer. Simul.* **2022**, *113*, 106581.
10. Wei, R.; Cao, J. Fixed-time synchronization of quaternion-valued memristive neural networks with time delays. *Neural Netw.* **2019**, *113*, 1–10.
11. Tu, Z.; Cao, J.; Hayat, T. Matrix measure based dissipativity analysis for inertial delayed uncertain neural networks. *Neural Netw.* **2016**, *75*, 47–55.
12. Cohen, M.A.; Grossberg, S. Absolute stability of global pattern formation and parallel memory storage by competitive neural networks. *IEEE Trans. Syst. Man Cybern.* **1983**, *13*, 815–826.
13. Zheng, C.; Hu, C.; Yu, J.; et al. Fixed-time synchronization of discontinuous competitive neural networks with time-varying delays. *Neural Netw.* **2022**, *153*, 192–203.
14. Lou, X.; Cui, B. Synchronization of competitive neural networks with different time scales. *Phys. A Stat. Mech. Its Appl.* **2007**, *380*, 563–576.
15. Duan, L.; Fang, X.; Yi, X.; et al. Finite-time synchronization of delayed competitive neural networks with discontinuous neuron activations. *Int. J. Mach. Learn. Cybern.* **2018**, *9*, 1649–1661.
16. Yang, X.; Li, C.; Song, Q.; et al. Global mittag-leffler stability and synchronization analysis of fractional-order quaternion-valued neural networks with linear threshold neurons. *Neural Netw.* **2018**, *105*, 88–103.
17. Pratap, A.; Raja, R.; Cao, J.; et al. Stability and synchronization criteria for fractional order competitive neural networks with time delays: An asymptotic expansion of mittag leffler function. *J. Frankl. Inst.* **2019**, *356*, 2212–2239.
18. Pecora, L.M.; Carroll, T.L. Synchronization in chaotic systems. *Phys. Rev. Lett.* **1990**, *64*, 821.
19. Wang, P.; Wen, G.; Yu, X.; et al. Synchronization of multi-layer networks: From node-to-node synchronization to complete synchronization. *IEEE Trans. Circuits Syst. I Regul. Pap.* **2018**, *66*, 1141–1152.
20. Guo, R. Projective synchronization of a class of chaotic systems by dynamic feedback control method. *Nonlinear Dyn.* **2017**, *90*, 53–64.
21. Zhang, G.; Hu, J.; Shen, Y. Exponential lag synchronization for delayed memristive recurrent neural networks. *Neurocomputing* **2015**, *154*, 86–93.
22. Petković, T.; Pribanić, T.; Đonlić, M.; et al. Software synchronization of projector and camera for structured light 3d body scanning. In Proceedings of the 7th International Conference on 3D Body Scanning Technologies, Lugano, Switzerland, 30 November–1 December 2016.
23. Gupta, H.; Jin, K.H.; Nguyen, H.Q.; et al. Cnn-based projected gradient descent for consistent ct image reconstruction. *IEEE Trans. Med. Imaging* **2018**, *37*, 1440–1453.
24. Liu, Y.; Wang, Z.; Ma, Q.; et al. Multistability analysis of delayed recurrent neural networks with a class of piecewise nonlinear activation functions. *Neural Netw.* **2022**, *152*, 80–89.
25. Ghosh, D. Time scale synchronization between two different time-delayed systems. *Electron. J. Theor. Phys.* **2009**, *6*, 125–138.
26. Yang, W.; Wang, Y.W.; Morărescu, I.C.; et al. Fixed-time synchronization of competitive neural networks with multiple time scales. *IEEE Trans. Neural Netw. Learn. Syst.* **2021**, *33*, 4133–4138.
27. Huang, Q.; Yu, Y.; Cao, J. Projective synchronization of inertial quaternion-valued neural networks via non-reduced order approach. *Neural Process. Lett.* **2024**, *56*, 21.
28. Kumar, R.; Sarkar, S.; Das, S.; et al. Projective synchronization of delayed neural networks with mismatched parameters and impulsive effects. *IEEE Trans. Neural Netw. Learn. Syst.* **2019**, *31*, 1211–1221.
29. Jiang, C.; Tang, Z.; Park, J.H.; et al. Matrix measure-based projective synchronization on coupled neural networks with clustering trees. *IEEE Trans. Cybern.* **2021**, *53*, 1222–1234.
30. Cloud, M.J.; Drachman, B.C.; Lebedev, L. *Inequalities*; Springer: Berlin/Heidelberg, Germany, 1998.
31. Peng, T.; Qiu, J.; Lu, J.; et al. Finite-time and fixed-time synchronization of quaternion-valued neural networks with/without mixed delays: An improved one-norm method. *IEEE Trans. Neural Netw. Learn. Syst.* **2021**, *33*, 7475–7487.
32. Liu, X.; Chen, T. Finite-time and fixed-time cluster synchronization with or without pinning control. *IEEE Trans. Cybern.* **2016**, *48*, 240–252.

33. Deng, H.; Bao, H. Fixed-time synchronization of quaternion-valued neural networks. *Phys. A Stat. Mech. Its Appl.* **2019**, *527*, 121351.
34. Aouiti, C.; Bessifi, M. Periodically intermittent control for finite-time synchronization of delayed quaternion-valued neural networks. *Neural Comput. Appl.* **2021**, *33*, 6527–6547.
35. Ansari, M.S.H.; Malik, M. Projective synchronization of fractional order quaternion valued uncertain competitive neural networks. *Chin. J. Phys.* **2024**, *88*, 740–755.